TRANSPLANTATION

Hematopoietic stem cell transplantation in immunocompetent hosts without radiation or chemotherapy

Akanksha Chhabra,[1]* Aaron M. Ring,[2,3,4]* Kipp Weiskopf,[2,3,4]* Peter John Schnorr,[1] Sydney Gordon,[2,3,4] Alan C. Le,[1] Hye-Sook Kwon,[1] Nan Guo Ring,[2,3,4] Jens Volkmer,[2,3,4] Po Yi Ho,[2,3,4] Serena Tseng,[2,3,4] Irving L. Weissman,[2,3,4,5] Judith A. Shizuru[1,2,3†]

Hematopoietic stem cell (HSC) transplantation can cure diverse diseases of the blood system, including hematologic malignancies, anemias, and autoimmune disorders. However, patients must undergo toxic conditioning regimens that use chemotherapy and/or radiation to eliminate host HSCs and enable donor HSC engraftment. Previous studies have shown that anti–c-Kit monoclonal antibodies deplete HSCs from bone marrow niches, allowing donor HSC engraftment in immunodeficient mice. We show that host HSC clearance is dependent on Fc-mediated antibody effector functions, and enhancing effector activity through blockade of CD47, a myeloid-specific immune checkpoint, extends anti–c-Kit conditioning to fully immunocompetent mice. The combined treatment leads to elimination of >99% of host HSCs and robust multilineage blood reconstitution after HSC transplantation. This targeted conditioning regimen that uses only biologic agents has the potential to transform the practice of HSC transplantation and enable its use in a wider spectrum of patients.

INTRODUCTION

Hematopoietic stem cells (HSCs) are multipotent stem cells that give rise to all cells of the blood system for the life of an individual (*1*). HSCs reside in specialized "niches" within the bone marrow that allow them to self-renew and remain in an undifferentiated state (*1*–*3*). Transplantation of HSCs into a host can regenerate a healthy blood system and, in so doing, cure many life-threatening blood disorders, autoimmune diseases, and hematologic malignancies. However, to achieve successful engraftment of exogenous HSCs, two obstacles must be overcome. First, donor HSCs must escape immune rejection by the recipient, and second, the transplanted cells must have access to niche space within the recipient bone marrow (*2*–*4*). The current conditioning regimens of radiation and/or chemotherapy simultaneously immunosuppress recipients by lymphoablation and elimination of resident HSCs to free bone marrow niches. However, these procedures also result in nonspecific injury to other tissues and can cause lifelong complications (*5*, *6*). Consequently, HSC transplantation is reserved for those with life-threatening disorders where the benefits are thought to outweigh the risks of the procedure. Safer and more targeted conditioning protocols could both improve the safety of transplantation and extend the existing clinical utility of this powerful form of cell therapy. Transplantation of purified allogeneic HSC has been shown in animal models to result in replacement of diseased hematopoietic cells without the complication of graft-versus-host disease (*7*). Pure HSC transplantations induce permanent transplantation tolerance of cells, tissues, or organs from the HSC donor and therefore represent a major platform upon which regenerative medicine rests (*8*).

HSCs and downstream hematopoietic progenitors express c-Kit (CD117), a dimeric transmembrane receptor tyrosine kinase (fig. S1) (*9*). Signaling engaged by c-Kit ligand (KL) is essential for numerous HSC functions, including homing, proliferation, adhesion, maintenance, and survival (*10*–*12*). The critical role of c-Kit in HSC regulation is evidenced in *W41/W41* mice that harbor hypomorphic *c-Kit* alleles. *W41/W41* mice have reduced numbers of HSCs (*13*) and can be robustly reconstituted by exogenous HSCs with minimal radiation (*14*). Similarly, immunocompromised *c-Kit* mutant mice can be used for allogeneic HSC transplantation (*15*) and engrafted by human HSCs (*16*) without any irradiation. Furthermore, targeted deletion of *KL* in perivascular cells results in loss of HSCs in vivo, thus establishing the requirement for KL in addition to the c-Kit receptor (*17*).

Administration of an anti-mouse c-Kit monoclonal antibody (mAb) (ACK2) into immunocompromised $Rag2^{-/-}\gamma c^{-/-}$ and $Rag2^{-/-}$ mice depletes host HSCs and enables exogenous HSCs to engraft (*18*). Similarly, administration of ACK2 in utero eliminates HSCs in developing mouse embryos and permits HSC engraftment in neonates (*19*). However, ACK2 as a single agent is incapable of conditioning immunocompetent adult mice to accept donor HSCs, and its combination with at least low-dose radiation is required for ACK2-mediated depletion of HSCs and engraftment in immunocompetent mice (*20*).

CD47, a transmembrane protein expressed on HSC and many other cell types, is a "don't eat me" signal that is an innate immune checkpoint and acts as a critical "marker of self" to attenuate antibody-dependent cell-mediated cytotoxicity/phagocytosis (ADCC/ADCP) via its interaction with SIRPα on neutrophils and macrophages (*21*–*23*). Mobilized or naturally circulating HSCs in peripheral blood up-regulate expression of surface CD47 to avoid destruction by macrophages in the perisinusoidal spaces in bone marrow, spleen, and liver (*24*). High levels of CD47 expression on many different cancer cells similarly confer protection of cancer cells from phagocytosis (*25*, *26*). Blockade of the CD47-SIRPα axis markedly enhances the ADCP activity of tumor-opsonizing mAbs in vitro and in vivo (*25*–*27*).

Here, we investigated whether CD47 antagonists can potentiate anti–c-Kit antibody–mediated HSC depletion. We show that selective targeting

[1]Blood and Marrow Transplantation, Stanford University School of Medicine, Stanford, CA 94305, USA. [2]Institute for Stem Cell Biology and Regenerative Medicine, Stanford University School of Medicine, Stanford, CA 94305, USA. [3]Stanford Cancer Institute, Stanford University School of Medicine, Stanford, CA 94305, USA. [4]Ludwig Center for Cancer Stem Cell Research and Medicine, Stanford University School of Medicine, Stanford, CA 94305, USA. [5]Department of Pathology, Stanford University Medical Center, Stanford, CA 94305, USA.
*These authors contributed equally to this work.
†Corresponding author. Email: jshizuru@stanford.edu

Downloaded from https://www.science.org at Fred Hutchinson Cancer Center on October 20, 2023

of c-Kit and CD47 with biologic agents only results in robust depletion of functional HSCs in immunocompetent recipients and permits engraftment of donor congenic HSCs. Furthermore, addition of T cell–depleting antibodies to achieve immune ablation in models of allogeneic HSC transplantation allowed robust HSC engraftment. These studies demonstrate a promising approach that has the potential to markedly improve the safety and broaden the use of HSC transplantation by targeted host conditioning, devoid of DNA-damaging agents.

RESULTS

Anti–c-Kit antibodies deplete HSCs in an Fc-dependent manner

We compared the ability of the anti–c-Kit antibody ACK2 to deplete HSCs in wild-type versus immunodeficient *Rag2*$^{-/-}c\gamma^{-/-}$ mice. As observed previously (*18*), ACK2-mediated depletion of immunophenotypic Lin$^-$Sca-1$^+$c-Kit$^+$CD150$^+$Flt3$^-$CD34$^-$ long-term HSCs (LT-HSCs) was greater in *Rag2*$^{-/-}c\gamma^{-/-}$ than in wild-type mice (Fig. 1A). In *Rag2*$^{-/-}c\gamma^{-/-}$ mice, a single 500-μg dose of ACK2 reduced LT-HSC numbers by greater than four orders of magnitude 6 days after administration. By contrast, in wild-type mice, ACK2 administration produced a modest (<10-fold) decrease in HSCs, with complete recovery of the HSC compartment 6 to 9 days later (Fig. 1A).

To determine whether the depletive activity of ACK2 could be enhanced in wild-type animals, we investigated the mechanism of ACK2-mediated HSC clearance. Previously, it was surmised that ACK2 acts primarily by blocking the interaction between c-Kit and KL based on studies that showed comparative lack of effectiveness of 2B8, a different nonblocking anti–c-Kit antibody (*18*, *28*), as well as similar loss of HSCs in the conditional *KL* knockout (*17*). However, multiple factors govern antibody efficacy, including Fc structural conformation and the ability to engage Fc receptors (FcRs) on host immune cells (*29*, *30*), which could also explain the differential activity of 2B8 versus ACK2. We thus examined whether ACK2 depletes HSC via effector cell involvement.

We addressed this question through multiple approaches. We prepared ACK2 Fab fragments, which lack antibody Fc. The Fc moiety plays a critical role in immune-mediated cell killing, including activation of effector cells and phagocytosis of target cells (*31*). Administration of intact ACK2 to *Rag2*$^{-/-}c\gamma^{-/-}$ mice caused the depletion of HSC in a dose-dependent manner. In contrast, Fab fragments of ACK2 had no discernible effect on HSC frequency, indicating that ACK2-mediated HSC depletion is dependent on its Fc portion (Fig. 1B). To further assess the Fc dependence of ACK2 for HSC depletion, we used *Fcer1g*$^{-/-}$ mice that are deficient in the γ-chain subunit of FcRIII, FcRI, and FcRIV. These mice lack functional ADCC activity of natural killer (NK) cells, phagocytic capacity of macrophages and neutrophils, and functional allergic activities of mast cells and basophils (*32*). Treatment of ACK2 in *Fcer1g*$^{-/-}$ mice had no effect on immunophenotypic HSC number in the bone marrow (Fig. 1C and fig. S2A), whereas a significant ($P = 0.0277$) but modest reduction was observed in wild-type mice (fig. S2B). The number of functional HSCs was similarly unaffected by ACK2 treatment in these mice, as determined by competitive transplantation analysis (fig. S2C). Because ACK2 has been previously demonstrated to effectively condition *Rag2*$^{-/-}c\gamma^{-/-}$ mice (*18*), we treated *Rag2*$^{-/-}c\gamma^{-/-}$ mice with the FcR blocking antibody 2.4G2 before ACK2 administration. Whereas ACK2-treated animals displayed increased granulocyte chimerism after HSC transplantation as compared to untreated controls, the 2.4G2

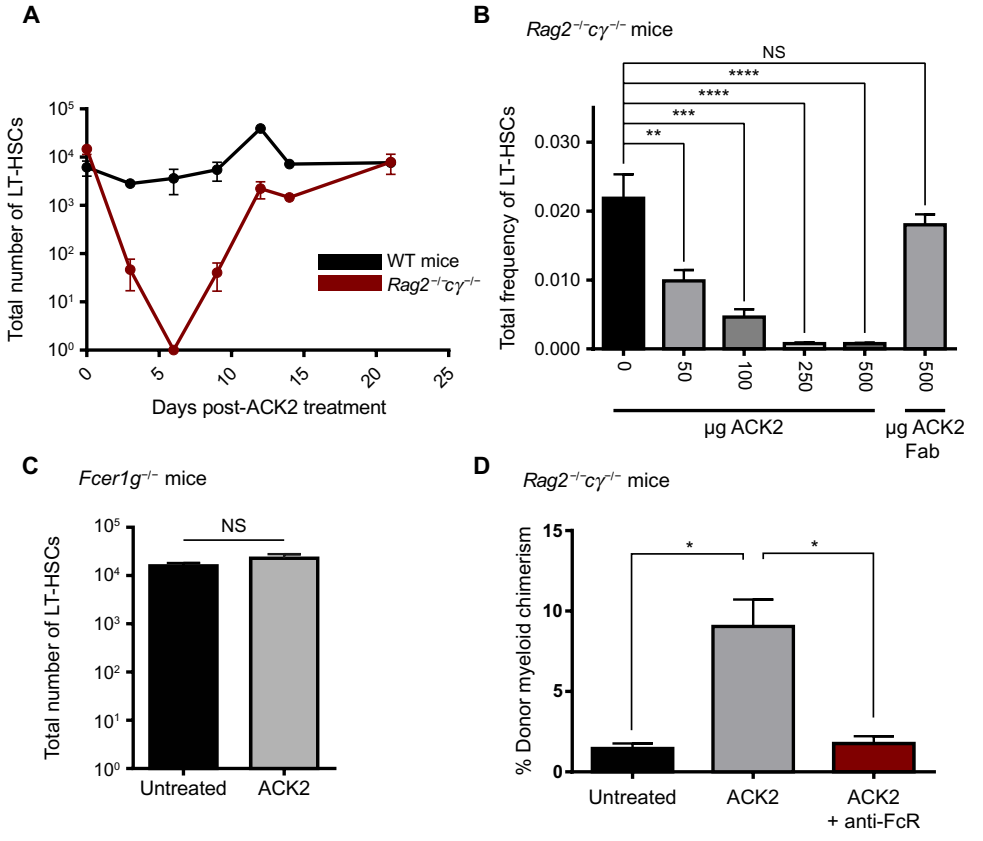

Fig. 1. Depletion of HSCs by anti–c-Kit antibody ACK2 is dependent on FcR activity. (**A**) Total number of phenotypic Lin$^-$c-Kit$^+$Sca-1$^+$CD150$^+$Flt3$^-$CD34$^-$ LT-HSCs in wild-type (WT) mice as compared to immunocompromised *Rag2*$^{-/-}c\gamma^{-/-}$ mice after treatment with anti–c-Kit antibody ACK2 ($n = 3$ to 5 per group; experiment was repeated three times). (**B**) Total frequency of Lin$^-$c-Kit$^+$Sca-1$^+$CD150$^+$Flt3$^-$CD34$^-$ LT-HSCs in *Rag2*$^{-/-}c\gamma^{-/-}$ mice 6 days after treatment with increasing concentrations of ACK2 compared to 500 μg of ACK2 Fab ($n = 3$ per group). (**C**) Number of Lin$^-$c-Kit$^+$Sca-1$^+$CD150$^+$Flt3$^-$CD34$^-$ LT-HSCs in *Fcer1g*$^{-/-}$ mice 6 days after ACK2 treatment as compared to untreated controls ($n = 3$; experiment was replicated in triplicate with similar results each time). (**D**) Frequency of donor-derived Mac-1$^+$Gr-1$^+$ granulocytes in peripheral blood of *Rag2*$^{-/-}c\gamma^{-/-}$ animals after either ACK2 treatment or FcR blocking before ACK2 as compared to untreated recipients. Data and error bars in (B) to (D) represent means ± SEM. NS, not significant; ****$P < 0.0001$, ***$P < 0.0005$, **$P < 0.005$, *$P < 0.05$.

Downloaded from https://www.science.org at Fred Hutchinson Cancer Center on October 20, 2023

blocking antibody inhibited this effect, demonstrating a general dependency on FcgRIIb and FcgRIII receptors (Fig. 1D). Furthermore, this effect was not due to a loss of effector cells, because 2.4G2 treatment alone did not cause reduction in myeloid cells in the peripheral blood, bone marrow, and spleen (fig. S3). Thus, removal of the Fc portion of ACK2 through preparation of Fab fragments, genetic deficiency of FcRs, and pharmacologic blockade of Fc-FcgRIIb and Fc-FcgRIII receptor interactions each abrogated the HSC-depletive activity of ACK2. Together, these results establish that antibody Fc effector functions elicited by ACK2 are necessary for its in vivo HSC-depletive activity.

CD47 blockade augments the efficacy of ACK2 for transplant conditioning

We previously demonstrated in mouse tumor models that blockade of the CD47-SIRPα axis markedly enhances the ADCP activity of antitumor antibodies (*27*). Hence, we hypothesized that interruption of the CD47-SIRPα interaction might similarly enhance depletion of endogenous HSCs using ACK2 or other anti–c-Kit antibodies. We therefore tested engineered fragments of human SIRPα as high-affinity antagonists of CD47 (*27*) or antibodies that block CD47 activity. The most potent of the high-affinity variants, CV1 (consensus variant 1), binds human CD47 (hCD47) with an affinity of 11 pM but cross-reacts more weakly with mouse CD47 (mCD47), with >1000-fold lower affinity than hCD47. We thus sought to redesign CV1 as an antagonist of mCD47 by fusing CV1 to the CH3 domain of human immunoglobulin G1 (IgG1) through a cysteine-containing hinge (Fig. 2A). Because the CH3 domain is homodimeric, the fusion protein exists as a disulfide-linked dimer of CV1 molecules. We reasoned that this new molecule, which we termed a CV1 "microbody" (CV1mb), would have enhanced affinity for mCD47 owing to the avidity afforded by its dimeric architecture. CV1mb efficiently blocked the SIRPα interface of CD47 on both human and mouse erythrocytes, as determined by competition with the blocking anti-hCD47 and anti-mCD47 mAbs Hu5F9-G4 and MIAP301, respectively (Fig. 2B). In vitro, CV1mb was functionally equivalent to monomeric CV1, because it induced no phagocytosis by itself but robustly synergized with an opsonizing mAb, cetuximab, which binds to the epidermal growth factor receptor (EGFR) present on a colon cancer cell line (Fig. 2C). We examined the in vivo duration of action of CV1 and CV1mb by measuring receptor occupancy, the ability to bind and block CD47. To assess the effect of the microbody format in extending the in vivo persistence of CV1, we administered CV1mb to mice and performed receptor occupancy studies of CD47 on mature mouse erythrocytes (which express high levels of CD47) at several time points after injection. Administration of a single dose (200 μg) of CV1mb to wild-type mice resulted in a

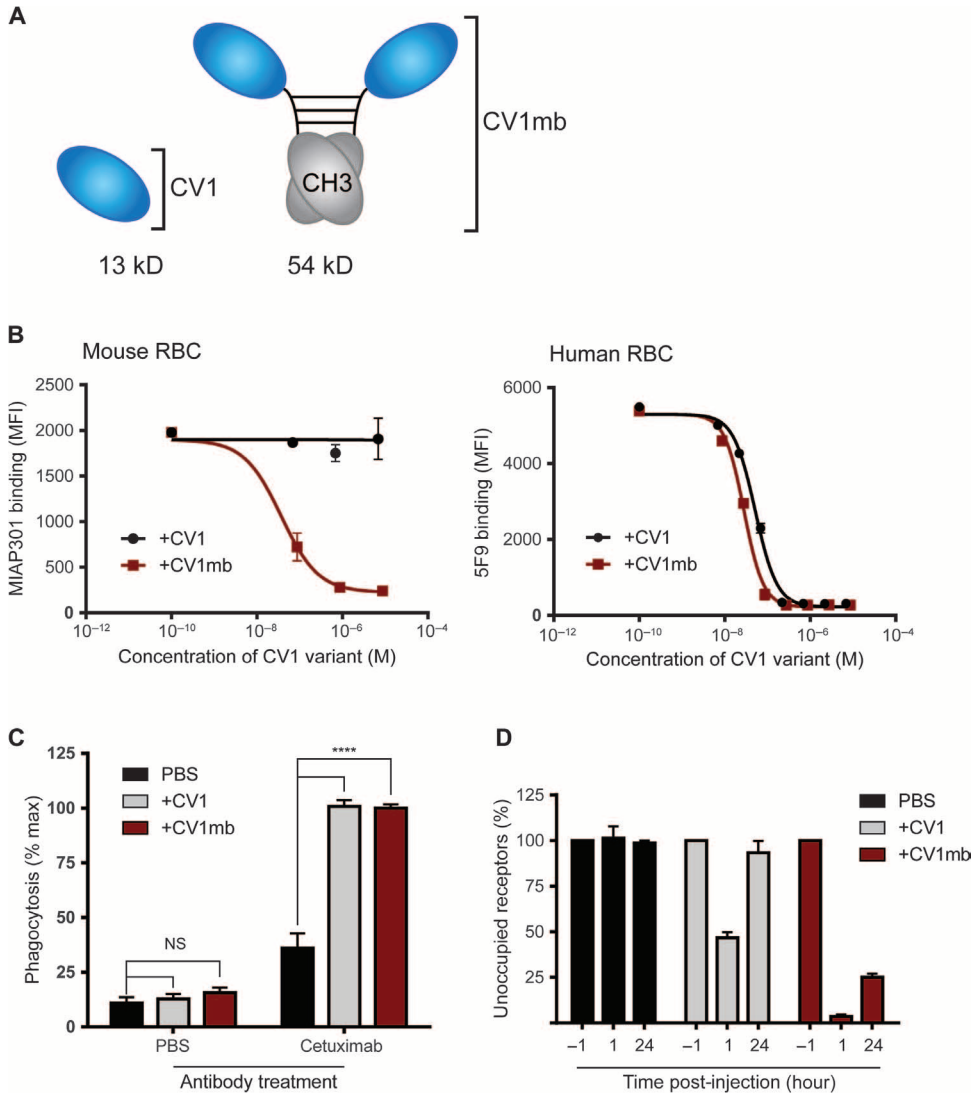

Fig. 2. Engineering a CV1mb as an antagonist of murine CD47. (**A**) Schematic of CV1 and CV1mb. CV1mb is a fusion of CV1 to the dimeric CH3 domain of human IgG1 linked by a disulfide-containing hinge. (**B**) Binding of CV1 and CV1mb to human and mouse blood, as determined by a flow cytometry–based receptor occupancy assay. Left: Blockade of allophycocyanin (APC)–labeled anti-mCD47 antibody MIAP301 binding to murine red blood cells (RBCs) by varying concentrations of CV1 and CV1mb. Right: Blockade of Alexa 488–labeled anti-hCD47 antibody Hu5F9-G4 binding to human RBCs by varying concentrations of CV1 and CV1mb. MFI, mean fluorescence intensity. (**C**) Phagocytosis of EGFR$^+$ DLD-1 colon cancer cells by human macrophages after treatment with cetuximab (anti-EGFR) with and without CV1 and CV1mb, indicated as a percentage of maximal response (seen in the CV1 + cetuximab treatment group). PBS, phosphate-buffered saline. (**D**) Erythrocyte CD47 receptor occupancy from mice administered 200 μg of CV1 or CV1mb measured 1 hour before, 1 hour after, and 24 hours after protein injection. Data and error bars in (B) to (D) represent means ± SEM. ****$P < 0.0001$. All experiments were repeated in duplicate.

Downloaded from https://www.science.org at Fred Hutchinson Cancer Center on October 20, 2023

more thorough and sustained occupancy of mCD47 on erythrocytes than an equivalent dose of CV1 monomer, blocking 96 and 75% of mCD47 after 1 and 24 hours versus 53 and 6% for CV1 monomer (Fig. 2D). Thus, the favorable binding, functional, and pharmacodynamic properties of CV1mb indicated that it could effectively antagonize mCD47 in vivo.

We then studied the effect of combining CD47 blockade using CV1mb with ACK2 treatment in immunocompetent C57BL/6.CD90.1 animals. As seen previously, administration of 500 μg of ACK2 alone in C57BL/6.CD90.1 failed to produce a sustained reduction of immunophenotypic HSCs after 7 days. Similarly, daily intraperitoneal injections for 5 days with 500 μg of CV1mb alone had no appreciable effect on immunophenotypic HSC numbers at the same time point. However, the combination of ACK2 and CV1mb resulted in a marked (>10,000-fold) reduction of $Lin^-Sca\text{-}1^+c\text{-}Kit^+$(LSK) $CD150^+$ $Flt3^-CD34^-$ LT-HSCs, as determined by flow cytometric analysis (Fig. 3A). To confirm that functional HSCs were eliminated, we cotransplanted whole bone marrow from ACK2/CV1mb-treated mice with an equal number of green fluorescent protein–positive (GFP^+) congenic bone marrow cells from unmanipulated mice into lethally irradiated recipients. HSC chimerism measured at 24 weeks after transplant was significantly reduced in recipients transplanted with bone marrow from ACK2 plus CV1mb–treated mice. In contrast, robust donor chimerism was observed in recipients of marrow from untreated and ACK2-treated mice (Fig. 3B).

Because c-Kit is expressed in the hematopoietic progenitor cells downstream of HSCs (fig. S1), we hypothesized that these populations might also be targeted by ACK2 combined with CV1mb. A significant loss of downstream myeloid progenitors was observed in mice treated with the combination of ACK2 and CV1mb (Fig. 3C). Accordingly, mice treated with combined ACK2 and CV1mb developed transient reduction of hematocrit, RBCs, and hemoglobin, as well as a decrease in white blood cells (fig. S4A). By histological examination, administration of ACK2 with CV1mb caused

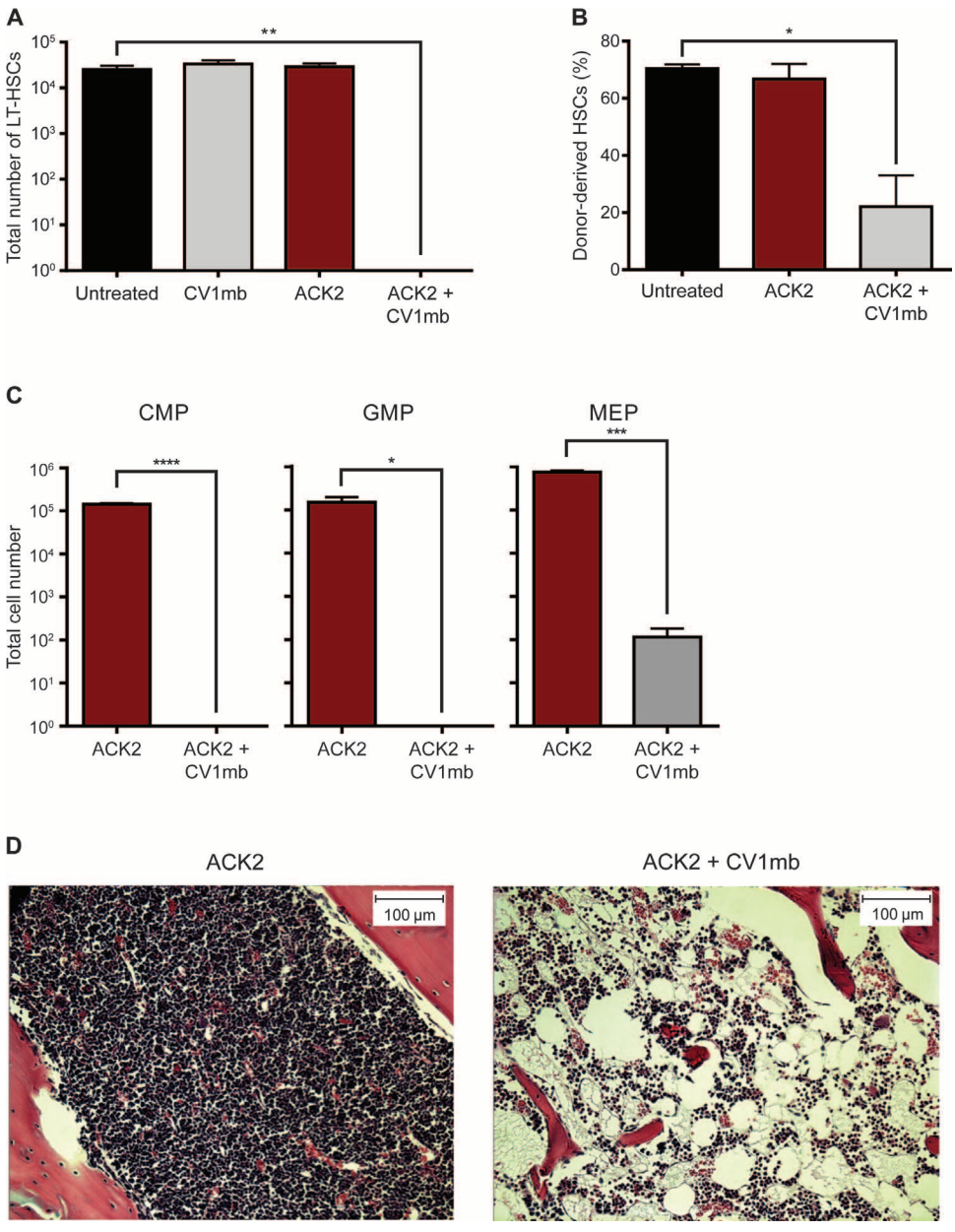

Fig. 3. Combining anti–c-Kit antibodies with CD47 blockade produces profound depletion of HSCs and clearance of the bone marrow niche in immunocompetent mice. (**A**) Total number of $Lin^-c\text{-}Kit^+Sca\text{-}1^+CD150^+Flt3^-CD34^-$ LT-HSCs in WT mice after 7 days of treatment with anti–c-Kit antibody ACK2, CD47 antagonist CV1mb, and combination of ACK2 and CV1mb as compared to untreated controls ($n = 3$; experiment was replicated four times). (**B**) Frequency of donor-derived HSCs in the bone marrow present 24 weeks after transplant into irradiated recipients. Recipients were transplanted with 1 million whole–bone marrow cells from treated donor mice and 1 million support bone marrow cells from GFP^+ donors ($n = 5$). (**C**) Total numbers of downstream myeloid progenitors are decreased 7 days after treatment with ACK2 and CV1mb as compared to ACK2 alone. CMP, common myeloid progenitor ($Lin^-Sca\text{-}1^+c\text{-}Kit^+FcRg^{lo}CD34^+$); GMP, granulocyte macrophage progenitor ($Lin^-Sca\text{-}1^-c\text{-}Kit^+FcRg^{hi}CD34^+$); MEP, megakaryocyte–erythroid progenitor ($Lin^-Sca\text{-}1^-c\text{-}Kit^+FcRg^{lo}CD34^-$). (**D**) Hematoxylin and eosin staining of bone marrow section depicting loss of bone marrow cellularity at 7 days in ACK2- and CV1mb-treated mice as compared to mice treated with ACK2 alone. Data and error bars in (B) to (D) represent means ± SEM. $^{****}P < 0.0001$, $^{***}P < 0.005$, $^{**}P < 0.01$, $^{*}P < 0.05$.

Downloaded from https://www.science.org at Fred Hutchinson Cancer Center on October 20, 2023

marked reduction of bone marrow cellularity. The clearance of the bone marrow by 7 days after treatment was characterized by a marked loss of mononuclear cells and RBCs revealing marrow adipocytes (Fig. 3D). This clearance of the bone marrow niche is distinct from the drastic angiectasis observed 7 days after lethal radiation (fig. S5). Notably, combined treatment of ACK2 plus CV1mb did not decrease functional HSCs in Fcer1g$^{-/-}$ mice (fig. S4B), as shown by no change in myeloid chimerism, indicating that the mechanism of the combined treatment regimen is dependent on FcR function. Thus, the near-complete depletion of HSCs and hematopoietic precursor cells and the apparent clearance of the bone marrow niche space by ACK2 plus CV1mb indicated that this combination could effectively precondition wild-type mice for HSC transplantation.

Preconditioning with ACK2 and CD47 blockade enables HSC transplantation in wild-type mice

To assess whether the combination of anti–c-Kit and CD47 blockade could permit donor HSC engraftment in the absence of chemotherapy or radiation, we treated fully immunocompetent C57Bl/6 CD45.1/CD45.2 adult mice with ACK2 and CV1mb and performed transplantation of lineage-depleted bone marrow cells (Fig. 4A). Whereas mice treated with ACK2 alone had very low levels of HSC engraftment, mice receiving the combination of ACK2 and CV1mb exhibited high levels of HSC engraftment 20 weeks after transplantation, about two orders of magnitude greater than the antibody alone (Fig. 4B). More than 60% donor-derived granulocyte chimerism was observed in the peripheral blood of ACK2- and CV1mb-treated mice (Fig. 4C), as well as in the bone marrow (fig. S6A) and spleen (fig. S6E). The engraftment was not limited to the myeloid compartment, because we observed an average of about 40 to 50% B cell (Fig. 4D), 30% T cell (Fig. 4F), and 60% NK cell donor chimerism in blood (Fig. 4E), as well as in the spleen (fig. S6, F to H) and bone marrow (fig. S6, B to D). The engraftment in the peripheral blood was relatively stable 12 weeks after transplant (fig. S7). T cell engraftment was also observed in the thymus (fig. S6I). In comparison with conditioning with radiation, we found that the combination of ACK2 and CV1mb was more effective than sublethal radiation with 250 or 450 cGy and equivalent to 750 cGy (fig. S8).

Given the robust synergism between ACK2 and CV1mb, we sought to determine whether conditioning with ACK2 could be generalized to other CD47 antagonists. We thus administered ACK2 with monomeric CV1 and an anti-CD47 antibody that blocks both mCD47 and hCD47 (MIAP410; fig. S9A). These combinations effectively enhanced ACK2-mediated depletion of functional HSCs similar to CV1mb, as determined by a competition transplant assay (fig. S9B). Furthermore, CV1 and MIAP410 enabled HSC transplantation when combined with ACK2 for conditioning, yielding 45 and 59% granulocyte chimerism, respectively (fig. S10A). B cell chimerism was moderate, with CV1 and ACK2 yielding 17% and MIAP410 combined with ACK2 resulting in 34% donor B cells (fig. S10B). T cell chimerism was low, with CV1 and ACK2 resulting in 7% and MIAP410 with ACK2 generating 8% (fig. S10C). These results indicate that pharmacologic CD47 blockade acts to potentiate the HSC-depletive activity of anti–c-Kit antibodies, and that the magnitude of the effect is influenced by the size, affinity/avidity, and/or antibody isotype of the CD47 antagonist. To confirm that the potent effect of ACK + MIAP410 is transient, we treated mice with this combination without HSC rescue and supported them at their hematopoietic nadir with whole-blood transfusions only. Under these conditions, recovery of the RBC lineage occurred at about 3 weeks after antibody treatment (fig. S11).

We wished to determine whether conditioning through the combination of anti–c-Kit antibody and CD47 antagonist could be extended to a clinically relevant model of allogeneic HSC transplantation, in which the donor and recipient are matched through human leukocyte antigen alleles but are mismatched at minor histocompatibility complex (mHC) antigens. Unlike radiation and chemotherapy, the combination of anti–c-Kit and CD47 blockade is unique in that it depletes HSC niches but is not expected to completely immunoablate recipients. Thus, we conditioned BALB/c mice with combinations of ACK2 and CV1mb or ACK2 and the anti-CD47 antibody MIAP410 in conjunction with immune ablation via T cell–depleting antibodies (anti-CD4 GK1.5 and anti-CD8 YTS169.4). The mice were subsequently transplanted with mHC-mismatched B10D2 sorted LSK HSCs (Fig. 5A). Neither ACK2 monotherapy nor treatment with anti-CD4/8 antibodies successfully conditioned recipient mice to accept allografted HSCs. However, when ACK + CV1mb or ACK2 + MIAP410 was combined with a T cell–depleting regimen of anti-CD4 and anti-CD8 antibodies, substantial granulocyte (Fig. 5C), B cell (Fig. 5D), T cell (Fig. 5E), and NK cell (fig. S5D) chimerism, as well as HSC engraftment (Fig. 5B) in the bone marrow, was observed. This multilineage chimerism was stable 12 weeks after transplant in the peripheral blood (fig. S12, A to C) and was significantly greater than untreated recipients (fig. S13, A to D). Multilineage chimerism was also present in the spleen (fig. S13, F to I), and T cell chimerism was observed in the thymus (fig. S13E). These results establish that a targeted, entirely biologic conditioning regimen free of DNA-damaging agents can promote stable purified HSC engraftment even in an allogeneic HSC transplant model.

DISCUSSION

A principal limitation of HSC transplantation remains the safe and facile liberation of the niche space to accept the donor graft. Our results establish that treatment of adult immunocompetent mice with two biologic agents, opsonizing anti–c-Kit antibodies and CD47 antagonists, leads to extensive depletion of HSC and progenitor cells and enables exogenous congenic HSCs to robustly engraft. Although previous studies have attempted to use ACK2 in immunocompetent recipients, it has not been possible without low-dose radiation. Combination of 300 cGy and 2 mg of ACK2 resulted in HSC chimerism (*20*), similar to our protocol of using ACK2 and CD47 antagonism. When additionally combined with transient depleting anti-lymphocyte antibodies, this regimen permitted HSC allotransplantation between mHC-mismatched donor/recipient pairs, the most common transplant scenario encountered clinically. The extension of this approach to humans could obviate the need for nonspecific toxic therapies that are the current standard of care and could subsequently allow for HSC transplantation to be extended to a broader set of patients. This prospect is particularly appealing in the era of modern gene-editing technologies, and it is readily conceivable that, for nonmalignant indications, a regimen consisting of anti–c-Kit plus CV1mb or anti-CD47 antibody such as Hu5F9G4, which is currently undergoing clinical trials (ClinicalTrials.gov NCT02216409 and NCT02367196), could enable autologous gene-edited HSC transplants to effectively cure inherited immunodeficiency, inborn errors of metabolism, hemoglobinopathies,

Downloaded from https://www.science.org at Fred Hutchinson Cancer Center on October 20, 2023

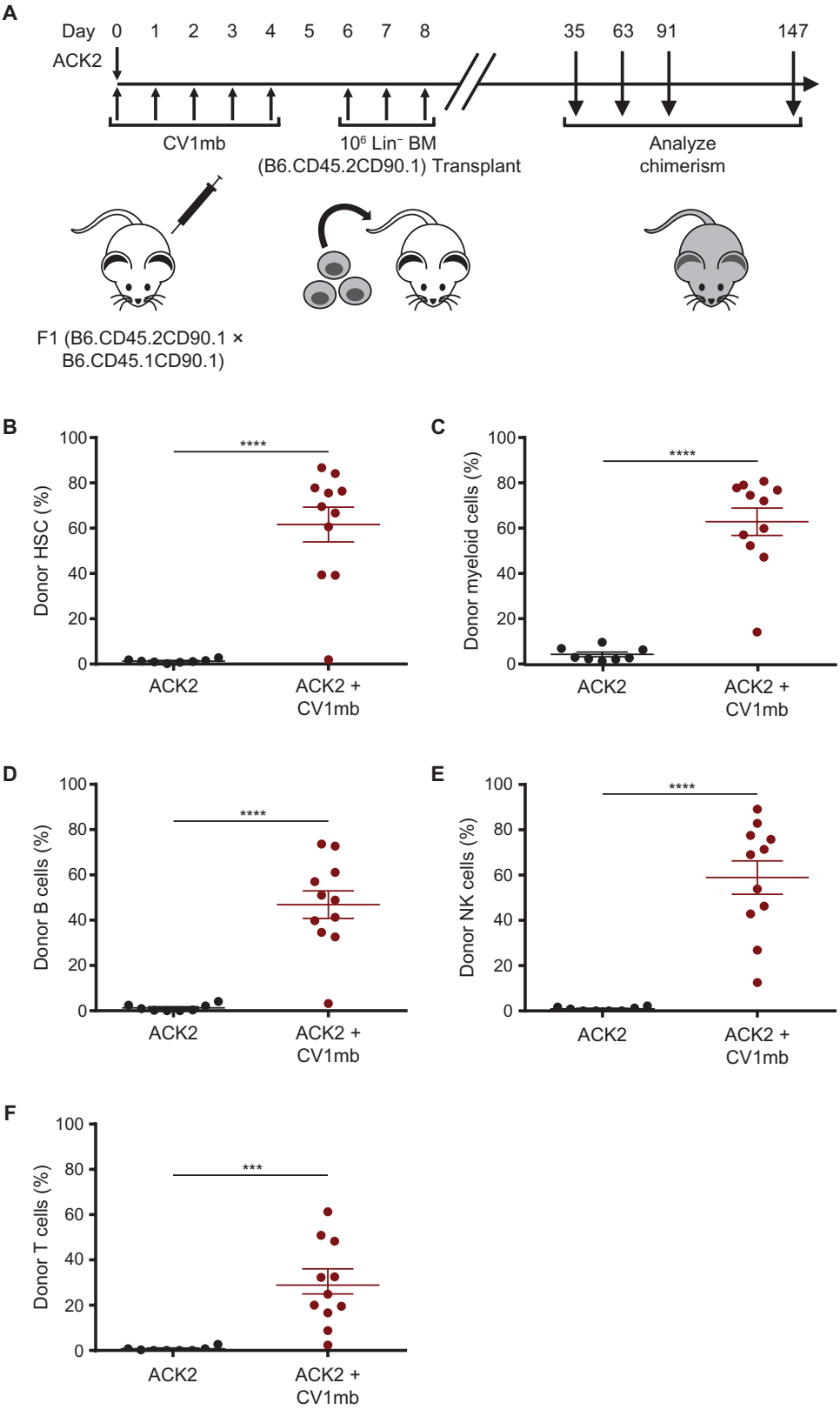

Fig. 4. Preconditioning with anti–c-Kit and CD47 blockade enables long-term engraftment of HSCs in immunocompetent mice. (**A**) Schematic of protocol for conditioning of recipients with anti–c-Kit antibody ACK2 and CD47 antagonist CV1mb. F1 mice expressing both CD45.1 and CD45.2 alleles were treated with 500 μg of ACK2 once and 500 μg of CV1mb daily for 5 days. Six days after treatment, 1 million CD45.2$^+$ donor Lin$^-$ cells were transplanted daily for 3 days (n = 3 to 5; experiment was replicated in triplicate). BM, bone marrow. (**B**) Frequency of donor-derived Lin$^-$c-Kit$^+$Sca-1$^+$CD150$^+$ HSCs in the bone marrow 24 weeks after transplant in ACK2- and CV1mb-treated recipients as compared to mice treated with ACK2 alone (n = 3 to 5; experiment was replicated in triplicate). (**C**) Donor-derived blood chimerism of Gr-1$^+$ Mac-1$^+$ myeloid cells. (**D**) Donor-derived blood chimerism of CD19$^+$ B cells. (**E**) Donor-derived blood chimerism of NK1.1$^+$ NK cells. (**F**) Donor-derived blood chimerism of CD3$^+$ T cells. All analyses were performed 24 weeks after transplant in ACK2- and CV1mb-treated recipients as compared to mice treated with ACK2 alone (n = 3 to 5; experiment was replicated in triplicate). Data and error bars in (B) to (F) represent means ± SEM. ****P < 0.0001, ***P < 0.005.

and other diseases, as well as induce tolerance for solid organ transplants.

The superior efficacy of ACK2 at HSC depletion in immunocompromised mice compared to immunocompetent wild-type mice is a question that remains incompletely resolved. Both T and B cells independently offer some protection from ACK2, suggesting two potential mechanisms for further study. One explanation may be that regulatory T cells regulate antibody-directed functions of macrophages, similar to their inhibition of antibody-dependent cytotoxicity of NK cells (*33*). Studies published by our group (*34*) and others (*35*) suggest that T cells influence HSC cycling in and out of the marrow niches. This effect of T cells is not due to their immune function per se, but rather appears to be related to the cytokines locally produced in the marrow. T cells may also exert control or suppression over the marrow macrophages. Similarly, B cells in wild-type mice may limit the effectiveness of ACK2 through the production of endogenous immunoglobulin, which could compete with ACK2 for binding to FcRs. This mechanism

Downloaded from https://www.science.org at Fred Hutchinson Cancer Center on October 20, 2023

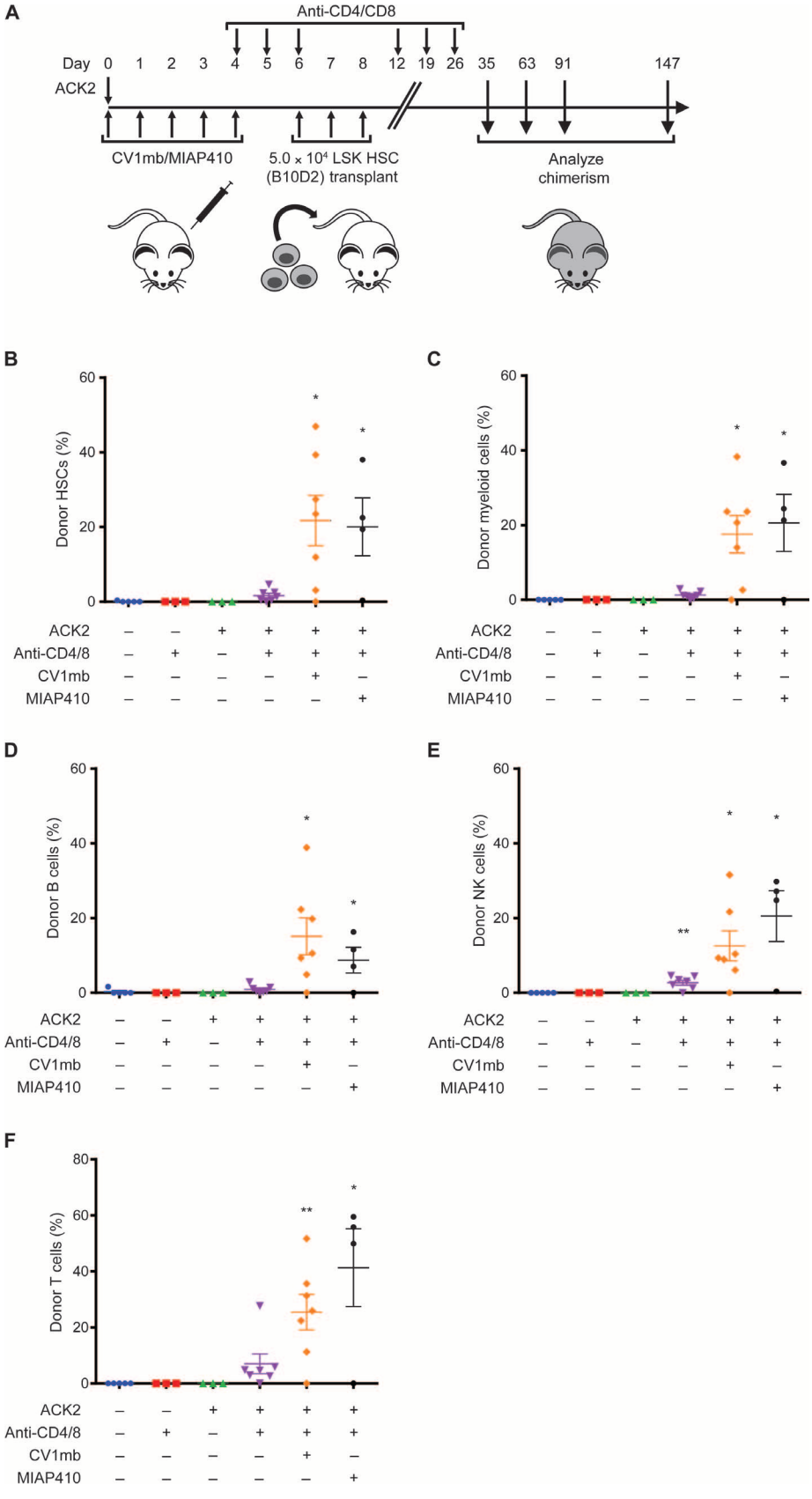

Fig. 5. HSC allotransplantation in an mHC-mismatched model by conditioning with anti–c-Kit, CD47 blockade, and lymphocyte-depleting antibodies. (**A**) Schematic of protocol for conditioning of recipients with anti–c-Kit antibody ACK2 and CD47 antagonist CV1mb or MIAP410. BALB/c mice expressing CD45.2 were treated with 500 μg of ACK2 once and 500 μg of CV1mb or MIAP410 daily for 5 days. Six days after treatment, 50,000 CD45.1$^+$ donor B10D2 LSK HSCs were transplanted daily for 3 days. CD4 (GK1.5) and CD8 (YTS169.4) T cell–depleting antibodies were administered starting 1 day before transplant and during the course of the transplant as described in Materials and Methods. (**B**) Frequency of donor-derived Lin$^-$c-Kit$^+$Sca-1$^+$CD150$^+$ HSCs in the bone marrow 24 weeks after transplant. (**C**) Donor-derived bone marrow chimerism of Gr-1$^+$Mac-1$^+$ myeloid cells. (**D**) Donor-derived bone marrow chimerism of CD19$^+$ B cells. (**E**) Donor-derived bone marrow chimerism of CD122$^+$Dx5$^+$ NK cells. (**F**) Donor-derived bone marrow chimerism of CD3$^+$ T cells. Data and error bars in (B) to (E) represent means ± SEM. $^{**}P < 0.01$, $^{*}P < 0.05$; significance is compared to untreated controls.

may be similar to the immunosuppressive effect elicited by administration of intravenous immunoglobulin. Irrespective of the cause of attenuated action of ACK2 in wild-type animals, the augmented efficacy of the antibody by CD47 blockade extends the treatment principle to a more realistic model of clinical practice.

The principal toxicity of cytopenias that we observed from the combined targeting of CD47 and c-Kit was secondary to stem and progenitor niche clearance, the intended consequence of this therapy. Mice receiving ACK2 + CD47 antagonists exhibited substantial reduction in hematologic parameters, particularly with respect to RBC indices. The half-life of RBCs in mice is shorter than that in humans (*36*), which may, in part, explain this effect. That said, in the clinical setting, this toxicity can be mitigated by careful monitoring and transient supportive transfusions. CD47-blocking therapies themselves can affect RBC indices, but dosing strategies have been described to avoid this toxicity (*37*). Furthermore, our studies use high doses of donor HSCs to achieve rapid blood cell recovery, a strategy that is clinically feasible as the numbers are similar to previously performed mega-dose CD34$^+$ cell transplants (*38*). c-Kit is widely expressed on other tissues. Hence, unwanted off-target effects are possible. However, to date, the reported side effects of ACK2 have been mild and transient, including graying of

Downloaded from https://www.science.org at Fred Hutchinson Cancer Center on October 20, 2023

mice (*18*) and reduction of spermatogonia (*19*). Although both CD47-blocking therapies and anti–c-Kit antibodies are being independently investigated in early-phase clinical trials, additional trials will be needed to assess the safety and feasibility of a combined regimen for patients.

Thus far, CD47 blockade has largely been applied to directing myeloid effector responses against cancers. The results presented here suggest a wider therapeutic application for blockade of the CD47-SIRPα pathway. The robust synergism between pharmacologic CD47 antagonism and anti–c-Kit antibodies in a syngeneic model provides strong evidence for the value of using CD47-blocking therapies to increase the cell-depletive capacity of therapeutic antibodies that target nonmalignant cells. The compelling therapeutic profile that anti–c-Kit antibodies combined with CD47 antagonism exhibited in allowing robust HSC engraftment suggests that such targeted therapy could supplant the toxic therapies that have traditionally been used to achieve HSC replacement in patients with disorders correctable with hematopoietic cell transplantations or HSC transplants.

MATERIALS AND METHODS

Protein expression and purification

CV1 was expressed and purified from BL21(DE3) *Escherichia coli* cells as previously described (*27*). For production of CV1mb, the CV1mb coding sequence was cloned in-frame with an N-terminal GP67 leader sequence and C-terminal 8× histidine tag into the baculovirus expression vector pAcGP67. Recombinant CV1mb baculovirus was prepared in Sf9 cells, and CV1mb protein was expressed by infection of Hi5 cells. Sixty hours after infection, secreted CV1mb was purified from the culture medium by nickel–nitrilotriacetic acid (Ni-NTA) chromatography. Endotoxin was removed by column washes with Triton X-114 as previously described. Purified proteins were desalted into PBS and passed through a sterile 0.22-μm filter.

Production and purification of ACK2 Fab fragments

Intact ACK2 antibody (a gift from S. Nishikawa) was digested using immobilized papain (Thermo Fisher) according to the manufacturer's instructions. Undigested ACK2 and Fc products were removed by passage of the reaction mixture over a protein A column, followed by ion exchange chromatography with a monoQ column. Purified Fab fragments were desalted into PBS and filtered with a 0.22-μm filter.

Mice

Mice used were 8- to 12-week-old, congenically distinguishable CD45.1, CD45.2, or CD45.1/CD45.2 C57Bl/6 or C57Bl/6.CD90.1 mice, *Rag2*$^{-/-}$*cγ*$^{-/-}$ mice, or *Fcer1g*$^{-/-}$ mice. All procedures were approved by the International Animal Care and Use Committee (protocol #12182). Mouse strains were bred and maintained at Stanford University's Research Animal Facility.

mCD47 and hCD47 antibody competition assays

For each sample, 1 μl of human or mouse blood was washed with fluorescence-activated cell sorting (FACS) buffer (PBS + 0.5 mM EDTA + 0.5% bovine serum albumin) and incubated with one of a range of concentrations (indicated in Fig. 3B) of either CV1 or CV1mb for 60 min on ice. After the samples were washed with FACS buffer to remove unbound CV1/CV1mb, unoccupied CD47 was detected by labeling with Alexa 488–conjugated Hu5F9-G4 (15 μg/ml) for human samples or APC-conjugated MIAP301 (15 μg/ml) (eBioscience) for murine samples on ice for 20 min. The samples were washed, and antibody staining was detected by flow cytometry with an LSRFortessa (BD). Data were analyzed using FlowJo (Tree Star) and fit to sigmoidal curves using Prism 6 (GraphPad).

Determination of erythrocyte CD47 occupancy from CV1/CV1mb-treated mice

Mice were treated with 200 μg of CV1 or CV1mb or PBS by intraperitoneal injection. One hour before, 1 hour after, and 24 hours after injection, 20 μl of blood was obtained through tail cut and collected into 200 μl of PBS with 10 mM EDTA (PBS-EDTA). The erythrocytes were then washed with FACS buffer and stained with anti-mCD47 antibody MIAP301 conjugated to Alexa 647 at a concentration of 40 μg/μl. Staining proceeded for 40 min on ice; the cells were then washed with FACS buffer and analyzed by flow cytometry with an LSRFortessa. Flow cytometry data were analyzed using FlowJo, and the percentage of unoccupied receptors was defined by the quotient of the background-subtracted MFI of each sample to the background-subtracted MFI in the absence of CD47 blockade. Data were plotted using Prism 6.

Phagocytosis assays

Human macrophages were differentiated as previously described (*27*). Briefly, leukocyte reduction system chambers were obtained from anonymous blood donors at the Stanford Blood Center. Monocytes were purified using whole-blood CD14 microbeads (Miltenyi), followed by separation using an autoMACS Pro Separator (Miltenyi). Monocytes were differentiated to macrophages by culture in Iscove's modified Dulbecco's medium (IMDM) with GlutaMAX (Thermo Fisher) plus 10% human AB serum (Gemini), penicillin (100 U/ml), and streptomycin (100 μg/ml) (Thermo Fisher) for 7 to 10 days. Macrophage phagocytosis of GFP$^+$ DLD-1 colon cancer cells was performed as previously described (*27*). Briefly, 50,000 macrophages and 100,000 GFP$^+$ DLD-1 cells were cocultured per well of a 96-well plate and incubated with the given treatments in serum-free IMDM at 37°C for 2 hours. The cell mixtures were then washed with autoMACS Running Buffer (Miltenyi) and stained with anti-CD45 (BioLegend) to label macrophages and 4′,6-diamidino-2-phenylindole (Sigma) to assess cell viability. Phagocytosis was determined by flow cytometry as the percentage of GFP$^+$ macrophages (CD45$^+$ cells) with an LSRFortessa. Flow cytometry data were analyzed using FlowJo and plotted in Prism 6 after normalization as the percentage of maximal phagocytosis. Statistical significance was determined in Prism by two-way analysis of variance (ANOVA) with correction for multiple comparisons.

Complete blood count analysis

Twenty microliters of whole blood per mouse was collected via the tail vein. Complete blood counts (CBCs) were conducted using Heska HemaTrue Veterinary Hematology Analyzer. For RBC parameter recovery, C57Bl/6.CD90.1 mice were treated with either ACK2 (500 μg) or ACK2 (500 μg) and five daily injections (500 μg each) of anti-CD47 antibody (MIAP410) and compared to untreated controls. Before ACK2, 400 μg of diphenhydramine (APP Pharmaceuticals, LLC) was injected via intraperitoneal injection. Day 0 was considered to be the time when the first injection of ACK2 or ACK2 + MIAP410 was administered. Combination-treated animals were given whole-blood transfusions (100 μl) from congenic animals as supportive care of day 6, 7, 8, and 10 post-ACK2 injection. Mice were bled twice weekly, and CBC analysis was performed.

Downloaded from https://www.science.org at Fred Hutchinson Cancer Center on October 20, 2023

Peripheral blood cell preparation for flow cytometry

About 100 μl of whole blood was collected via the tail vein. Blood was incubated on 2% dextran in PBS for 45 min at 37°C. Supernatant was extracted and lysed in ACK lysis buffer for 7 min on ice.

Bone marrow cell preparation

Mice were euthanized, and femurs and tibias were collected. Bones were crushed in PBS supplemented with 2% heat-inactivated fetal bovine serum (FBS). Cells were filtered through a 70-μm filter (Falcon). Bone marrow cells were lysed in ACK lysis buffer for 7 min on ice. Cells were filtered through a 70-μm filter (Falcon) and then counted on a Countess automated cell counter (Invitrogen).

Lineage-negative cell isolation from bone marrow for transplant

Mice were euthanized, and femurs, tibias, humeri, and coxa bones were collected. Bones were crushed in PBS supplemented with 2% heat-inactivated FBS. Cells were filtered through a 70-μm filter (Falcon). Bone marrow cells were lysed in ACK lysis buffer for 7 min on ice. Cells were filtered through a 70-μm filter (Falcon) and then counted on a Countess automated cell counter (Invitrogen). Lineage cell depletions were performed using Miltenyi Lineage Cell Depletion Kit according to the manufacturer's instructions.

Spleen and thymus cell preparation for staining and analysis

Spleens and thymi were directly mashed in a 70-μm filter with the plunger of a 3-ml syringe. Cells were lysed in ACK lysis buffer for 7 min on ice. Cells were filtered through a 70-μm filter (Falcon) and then counted on a Countess automated cell counter (Invitrogen).

Flow cytometry

All stainings were performed in 2% FBS for 20 to 45 min on ice. Cells were stained with optimal dilutions of eBioscience antibodies. Reagents used were as follows: Mac-1 phycoerythrin (PE)–Cy7 (M1/70), Mac-1 APC-Cy5 (M1/70), Mac-1 BV421 (M1/70), Mac-1 PE (M1/70), Gr-1 PE (RB6-8C5), GR-1 fluorescein isothiocyanate (FITC) (RB6-8C5), GR-1 BV421 (RB6-8C5), GR-1 PE (RB6-8C5), CD19 PE (ebio103), CD3 APC-Cy7 (17A2), CD45.1 APC (A20), CD45.1 BV421 (A20), CD45.1 APC (A20), CD45.2 APC (104), CD45.2 FITC (104), CD45.2 BV421 (104), B220 PE-Cy7 (RA3-6B2), B220 PE (RA3-6B2), B220 BV421 (RA3-6B2), NK1.1 FITC (PK136), Nk1.1 Pe-Cy7 (PK136), TCRβ APC (H57-597), Thy1.1 Pe-Cy7 (HISS1), CD4 PE (GK1.5), CD4 BV421 (GK1.5), CD8a PE (53-6.7), CD8a BV421 (53-6.7), SCA1 Pe-Cy7 (D7), CD117 APC-Cy7 (2B8), CD117 APC (2B8), CD150 BV421 (TC15-12 F 12.2), CD135 APC (A2F10), CD34 FITC (RAM34), CD16/32 PE (93), CD34, CD127 BV421 (A7R34), CD3 PE (17A2), CD3 BV421 (17A2), CD5 PE (53-7.3), CD5 BV421 (53-7.3), Ter119 PE (TER119), and Ter119 BV421 (TER119). Propidium iodide was used to distinguish between live and dead cells. Cells were analyzed on BD LSRII at the Stanford Shared FACS Facility. Data were analyzed using FlowJo 9.5 (Tree Star). Statistical significance was determined in Prism by two-way ANOVA with correction for multiple comparisons.

Bone marrow transplant

Mice were given retro-orbital injections of one of the following cell preparations that were resuspended in 100 μl of PBS: lineage-negative bone marrow cells, sorted LSK HSCs, or whole bone marrow. For competitive transplantation assays to determine functional HSCs, whole bone marrow of treated mice was mixed with equal numbers of congenic support whole bone marrow differing in CD45 allele expression and transplanted into recipients after lethal radiation was performed in split dose. Also, for competitive transplants with CV1mb- and ACK2-treated animals, whole bone marrow of treated mice was mixed with equal numbers of congenic GFP^+ support whole bone marrow. For FcR blocking transplants, $Rag2^{-/-}c\gamma^{-/-}$ were given 250 μg of 2.4G2, followed by 500 μg of ACK2 the next day along with 250 μg of 2.4G2 simultaneously. Before ACK2, 400 μg of diphenhydramine (APP Pharmaceuticals, LLC) was injected via intraperitoneal injection. The mice were given a total of seven injections of 2.4G2, 48 hours after the last 2.4G2 injection, 50,000 congenic B6.CD45.1 LSK HSCs were transplanted for three consecutive days. For ACK2 and CD47 antagonist congenic transplants, a single dose (500 μg) of ACK2 on day 0 and 500 μg of CV1mb/CV1/MIAP410 (a gift from I. Weissman) on day 0 followed by four daily injections of 500 μg of CV1mb/CV1/MIAP410 on days 1, 2, 3, and 4. Starting on day 6 after treatment, lineage-depleted $CD45.2^+$ bone marrow cells were transplanted daily for three consecutive days. For minor mismatch transplants, 50,000 sorted LSK HSCs were transplanted daily for 3 days. GK1.5 anti-CD4 (100 μg) (Bio X Cell) and YTS169.4 anti-CD8 (100 μg) (Bio X Cell) were administered by intraperitoneal injection starting 2 days before transplant for 3 days, and 4 days after the last transplant, followed by a single injection a week later, for 2 weeks. For comparison of radiation and ACK2 + CV1mb, 50,000 sorted LSK HSCs were transplanted daily for 3 days, 12 hours after radiation, or 6 days after initial ACK2 treatment.

Bone marrow histology

Femurs were dissected and fixed in 10% buffered formalin overnight. Bones were subsequently decalcified using Immunocal (Immunotec). Paraffin embedding and sectioning were performed by Histo-Tec Laboratory.

Statistical analysis

All analyses were performed using GraphPad Prism software, and *P* value was calculated using *t* test unless otherwise noted. Original data for all graphs are provided in table S1.

SUPPLEMENTARY MATERIALS

www.sciencetranslationalmedicine.org/cgi/content/full/8/351/351ra105/DC1

Fig. S1. Expression of c-Kit during hematopoiesis.

Fig. S2. ACK2 treatment does not affect functional HSC levels in $Fcer1g^{-/-}$ mice.

Fig. S3. FcgRIIb and FcgRIII blocking antibody 2.4G2 treatment alone does not deplete effector cells in $Rag2^{-/-}c\gamma^{-/-}$ mice.

Fig. S4. Anti–c-Kit antibody and CD47 antagonism suppress peripheral blood counts and are dependent on FcR function.

Fig. S5. Bone marrow composition after various doses of radiation.

Fig. S6. Preconditioning with anti–c-Kit and CV1mb enables long-term multilineage congenic hematopoietic engraftment in immunocompetent mice 20 weeks after transplantation.

Fig. S7. Preconditioning with anti–c-Kit and CV1mb enables stable multilineage chimerism in peripheral blood.

Fig. S8. Comparison of conditioning by combined anti–c-Kit and CD47 blockade versus radiation.

Fig. S9. Anti–c-Kit antibody ACK2 combined with additional CD47-blocking reagents enhances depletion of functional HSC in immunocompetent mice.

Fig. S10. Anti–c-Kit antibody ACK2 combined with additional CD47-blocking reagents enables granulocyte and lymphoid chimerism in transplanted immunocompetent recipients.

Fig. S11. Transient depletion of RBC parameters is observed using the combination of ACK2 and anti-CD47 antibody.

Fig. S12. Preconditioning with anti–c-Kit and anti-CD47 in combination with T cell–depleting antibodies enables stable multilineage chimerism in peripheral blood in an mHC-mismatched model of HSC allotransplantation.

Downloaded from https://www.science.org at Fred Hutchinson Cancer Center on October 20, 2023

Fig. S13. Preconditioning with anti–c-Kit, anti-CD47, and T cell–depleting antibodies enables long-term multilineage chimerism in immunocompetent mice 24 weeks after transplantation in an mHC-mismatched model of HSC allotransplantation.
Table S1. Source data.

REFERENCES AND NOTES

1. J. A. Shizuru, R. S. Negrin, I. L. Weissman, Hematopoietic stem and progenitor cells: Clinical and preclinical regeneration of the hematolymphoid system. *Annu. Rev. Med.* **56**, 509–538 (2005).
2. C. K. F. Chan, C.-C. Chen, C. A. Luppen, J.-B. Kim, A. T. DeBoer, K. Wei, J. A. Helms, C. J. Kuo, D. L. Kraft, I. L. Weissman, Endochondral ossification is required for haematopoietic stem-cell niche formation. *Nature* **457**, 490–494 (2009).
3. C. K. F. Chan, E. Y. Seo, J. Y. Chen, D. Lo, A. McArdle, R. Sinha, R. Tevlin, J. Seita, J. Vincent-Tompkins, T. Wearda, W.-J. Lu, K. Senarath-Yapa, M. T. Chung, O. Marecic, M. Tran, K. S. Yan, R. Upton, G. G. Walmsley, A. S. Lee, D. Sahoo, C. J. Kuo, I. L. Weissman, M. T. Longaker, Identification and specification of the mouse skeletal stem cell. *Cell* **160**, 285–298 (2015).
4. D. Bhattacharya, L. I. Ehrlich, I. L. Weissman, Space-time considerations for hematopoietic stem cell transplantation. *Eur. J. Immunol.* **38**, 2060–2067 (2008).
5. H. J. Deeg; Seattle Marrow Transplant Team, Acute and delayed toxicities of total body irradiation. *Int. J. Radiat. Oncol. Biol. Phys.* **9**, 1933–1939 (1983).
6. G. Socié, N. Salooja, A. Cohen, A. Rovelli, E. Carreras, A. Locasciulli, E. Korthof, J. Weis, V. Levy, A. Tichelli; Late Effects Working Party of the European Study Group for Blood and Marrow Transplantation, Nonmalignant late effects after allogeneic stem cell transplantation. *Blood* **101**, 3373–3385 (2003).
7. J. A. Shizuru, L. Jerabek, C. T. Edwards, I. L. Weissman, Transplantation of purified hematopoietic stem cells: Requirements for overcoming the barriers of allogeneic engraftment. *Biol. Blood Marrow Transplant.* **2**, 3–14 (1996).
8. I. Weissman, Stem Cell Research: Paths to cancer therapies and regenerative medicine. *JAMA* **294**, 1359–1366 (2005).
9. S. Okada, H. Nakauchi, K. Nagayoshi, S. Nishikawa, S. Nishikawa, Y. Miura, T. Suda, Enrichment and characterization of murine hematopoietic stem cells that express c-kit molecule. *Blood* **78**, 1706–1712 (1991).
10. D. Kent, M. Copley, C. Benz, B. Dykstra, M. Bowie, C. Eaves, Regulation of hematopoietic stem cells by the steel factor/KIT signaling pathway. *Clin. Cancer Res.* **14**, 1926–1930 (2008).
11. J. Domen, I. L. Weissman, Hematopoietic stem cells need two signals to prevent apoptosis; BCL-2 can provide one of these, Kitl/c-Kit signaling the other. *J. Exp. Med.* **192**, 1707–1718 (2000).
12. E. A. McCulloch, L. Siminovitch, J. E. Till, Spleen-colony formation in anemic mice of genotype WW. *Science* **144**, 844–846 (1964).
13. L. A. Thorén, K. Liuba, D. Bryder, J. M. Nygren, C. T. Jensen, H. Qian, J. Antonchuk, S.-E. W. Jacobsen, Kit regulates maintenance of quiescent hematopoietic stem cells. *J. Immunol.* **180**, 2045–2053 (2008).
14. S. L. Hall, K.-H. W. Lau, S.-T. Chen, J. C. Felt, D. S. Gridley, J.-K. Yee, D. J. Baylink, An improved mouse Sca-1+ cell-based bone marrow transplantation model for use in gene- and cell-based therapeutic studies. *Acta Haematol.* **117**, 24–33 (2007).
15. C. Waskow, V. Madan, S. Bartels, C. Costa, R. Blasig, H.-R. Rodewald, Hematopoietic stem cell transplantation without irradiation. *Nat. Methods* **6**, 267–269 (2009).
16. K. N. Cosgun, S. Rahmig, N. Mende, S. Reinke, I. Hauber, C. Schäfer, A. Petzold, H. Weisbach, G. Heidkamp, A. Purbojo, R. Cesnjevar, A. Platz, M. Bornhäuser, M. Schmitz, D. Dudziak, J. Hauber, J. Kirberg, C. Waskow, Kit regulates HSC engraftment across the human-mouse species barrier. *Cell Stem Cell* **15**, 227–238 (2014).
17. L. Ding, T. L. Saunders, G. Enikolopov, S. J. Morrison, Endothelial and perivascular cells maintain haematopoietic stem cells. *Nature* **481**, 457–462 (2012).
18. A. Czechowicz, D. Kraft, I. L. Weissman, D. Bhattacharya, Efficient transplantation via antibody-based clearance of hematopoietic stem cell niches. *Science* **318**, 1296–1299 (2007).
19. S. C. Derderian, P. P. Togarrati, C. King, P. W. Moradi, D. Reynaud, A. Czechowicz, I. L. Weissman, T. C. MacKenzie, In utero depletion of fetal hematopoietic stem cells improves engraftment after neonatal transplantation in mice. *Blood* **124**, 973–980 (2014).
20. X. Xue, N. K. Pech, W. C. Shelley, E. F. Srour, M. C. Yoder, M. C. Dinauer, Antibody targeting KIT as pretransplantation conditioning in immunocompetent mice. *Blood* **116**, 5419–5422 (2010).
21. M. P. Chao, R. Majeti, I. L. Weissman, Programmed cell removal: A new obstacle in the road to developing cancer. *Nat. Rev. Cancer* **12**, 58–67 (2012).
22. P. Jiang, C. F. Lagenaur, V. Narayanan, Integrin-associated protein is a ligand for the P84 neural adhesion molecule. *J. Biol. Chem.* **274**, 559–562 (1999).
23. E. J. Brown, W. A. Frazier, Integrin-associated protein (CD47) and its ligands. *Trends Cell Biol.* **11**, 130–135 (2001).
24. S. Jaiswal, C. H. M. Jamieson, W. W. Pang, C. Y. Park, M. P. Chao, R. Majeti, D. Traver, N. van Rooijen, I. L. Weissman, CD47 is upregulated on circulating hematopoietic stem cells and leukemia cells to avoid phagocytosis. *Cell* **138**, 271–285 (2009).
25. R. Majeti, M. P. Chao, A. A. Alizadeh, W. W. Pang, S. Jaiswal, K. D. Gibbs Jr., N. van Rooijen, I. L. Weissman, CD47 is an adverse prognostic factor and therapeutic antibody target on human acute myeloid leukemia stem cells. *Cell* **138**, 286–299 (2009).
26. S. B. Willingham, J.-P. Volkmer, A. J. Gentles, D. Sahoo, P. Dalerba, S. S. Mitra, J. Wang, H. Contreras-Trujillo, R. Martin, J. D. Cohen, P. Lovelace, F. A. Scheeren, M. P. Chao, K. Weiskopf, C. Tang, A. K. Volkmer, T. J. Naik, T. A. Storm, A. R. Mosley, B. Edris, S. M. Schmid, C. K. Sun, M.-S. Chua, O. Murillo, P. Rajendran, A. C. Cha, R. K. Chin, D. Kim, M. Adorno, T. Raveh, D. Tseng, S. Jaiswal, P. Ø. Enger, G. K. Steinberg, G. Li, S. K. So, R. Majeti, G. R. Harsh, M. van de Rijn, N. N. Teng, J. B. Sunwoo, A. A. Alizadeh, M. F. Clarke, I. L. Weissman, The CD47-signal regulatory protein alpha (SIRPa) interaction is a therapeutic target for human solid tumors. *Proc. Natl. Acad. Sci. U.S.A.* **109**, 6662–6667 (2012).
27. K. Weiskopf, A. M. Ring, C. C. M. Ho, J.-P. Volkmer, A. M. Levin, A. K. Volkmer, E. Özkan, N. B. Fernhoff, M. van de Rijn, I. L. Weissman, K. C. Garcia, Engineered SIRPα variants as immunotherapeutic adjuvants to anticancer antibodies. *Science* **341**, 88–91 (2013).
28. M. Okura, H. Maeda, S.-i. Nishikawa, M. Mizoguchi, Effects of monoclonal anti-c-kit antibody (ACK2) on melanocytes in newborn mice. *J. Invest. Dermatol.* **105**, 322–328 (1995).
29. A. Pincetic, S. Bournazos, D. J. DiLillo, J. Maamary, T. T. Wang, R. Dahan, B.-M. Fiebiger, J. V. Ravetch, Type I and type II Fc receptors regulate innate and adaptive immunity. *Nat. Immunol.* **15**, 707–716 (2014).
30. D. J. DiLillo, J. V. Ravetch, Fc-receptor interactions regulate both cytotoxic and immunomodulatory therapeutic antibody effector functions. *Cancer Immunol. Res.* **3**, 704–713 (2015).
31. A. M. Scott, J. D. Wolchok, L. J. Old, Antibody therapy of cancer. *Nat. Rev. Cancer* **12**, 278–287 (2012).
32. T. Takai, M. Li, D. Sylvestre, R. Clynes, J. V. Ravetch, FcR γ chain deletion results in pleiotrophic effector cell defects. *Cell* **76**, 519–529 (1994).
33. P. Trzonkowski, E. Szmit, J. Myśliwska, A. Dobyszuk, A. Myśliwski, $CD4^+CD25^+$ T regulatory cells inhibit cytotoxic activity of T $CD8^+$ and NK lymphocytes in the direct cell-to-cell interaction. *Clin. Immunol.* **112**, 258–267 (2004).
34. A. M. S. Müller, J. Poyser, N. J. Küpper, C. Burnett, R. M. Ko, H. E. Kohrt, M. Florek, P. Zhang, R. S. Negrin, J. A. Shizuru, Donor hematopoiesis in mice following total lymphoid irradiation requires host T-regulatory cells for durable engraftment. *Blood* **123**, 2882–2892 (2014).
35. M. T. Baldridge, K. Y. King, N. C. Boles, D. C. Weksberg, M. A. Goodell, Quiescent haematopoietic stem cells are activated by IFN-γ in response to chronic infection. *Nature* **465**, 793–797 (2010).
36. M. Magnani, L. Rossi, V. Stocchi, L. Cucchiarini, G. Piacentini, G. Fornaini, Effect of age on some properties of mice erythrocytes. *Mech. Ageing Dev.* **42**, 37–47 (1988).
37. J. Liu, L. Wang, F. Zhao, S. Tseng, C. Narayanan, L. Shura, S. Willingham, M. Howard, S. Prohaska, J. Volkmer, M. Chao, I. L. Weissman, R. Majeti, Pre-clinical development of a humanized anti-CD47 antibody with anti-cancer therapeutic potential. *PLOS One* **10**, e0137345 (2015).
38. C. C. Dvorak, A. L. Gilman, B. Horn, C.-Y. Oon, E. A. Dunn, L. A. Baxter-Lowe, M. J. Cowan, Haploidentical related-donor hematopoietic cell transplantation in children using megadoses of CliniMACs-selected $CD34^+$ cells and a fixed $CD3^+$ dose. *Bone Marrow Transplant.* **48**, 508–513 (2013).

Acknowledgments: We thank members of the Shizuru and Weissman laboratory for helpful advice, critical discussion, and technical assistance. We thank the Stanford Shared FACS Facility. **Funding:** This study was supported by the Virginia and D.K. Ludwig Fund for Cancer Research, the California Institute for Regenerative Medicine (grant RT3-07683 to I.L.W. and J.A.S. and grant DR2A-05365 to J.A.S.), the NIH (grants R01 CA86065 and R01HL058770 to I.L.W.), Stanford Medical Scientist Training Program (NIH-GM07365 to K.W. and A.M.R.), a Siebel Fellowship from the Thomas and Stacey Siebel Foundation (to I.L.W.), the Gunn/Olivier Research Fund (to I.L.W. and J.A.S.), the HL Snyder Medical Foundation (to J.A.S.), and the Stinehart-Reed Foundation (to J.A.S.). **Author contributions:** A.M.R., K.W., and A.C. designed the studies and wrote the manuscript. A.C. and P.J.S. designed experiments, conducted in vivo studies, and analyzed data. A.C.L. and H.-S.K. provided technical assistance. A.C. and H.-S.K. performed depletion studies on immunocompromised mice. P.J.S. and H.-S.K. edited the manuscript. A.C.L. prepared final figures for publication. A.M.R. designed CV1mb, prepared Fab fragments of ACK2, and produced CV1. A.M.R. and S.G. produced CV1mb for in vitro and in vivo studies. N.G.R. performed phagocytosis assays. P.Y.H. and S.T. conducted pharmacokinetic studies. J.V., A.M.R., and K.W. performed receptor occupancy assays. I.L.W. and J.A.S. supervised the project and edited the manuscript. **Competing interests:** A.M.R., A.C., K.W., P.J.S., J.A.S., and I.L.W. are inventors on the patent described by the article (U.S. Patent 62/041,989). K.W., A.M.R., J.V., and I.L.W. are cofounders of Forty Seven Inc., the company that licensed the technology for radiation- and chemotherapy-free HSC transplantation. K.W. and A.M.R. have advised Alexo Therapeutics, a company that develops CD47-based therapeutics.

Submitted 9 December 2015
Accepted 15 July 2016
Published 10 August 2016
10.1126/scitranslmed.aae0501

Citation: A. Chhabra, A. M. Ring, K. Weiskopf, P. J. Schnorr, S. Gordon, A. C. Le, H.-S. Kwon, N. G. Ring, J. Volkmer, P. Y. Ho, S. Tseng, I. L. Weissman, J. A. Shizuru, Hematopoietic stem cell transplantation in immunocompetent hosts without radiation or chemotherapy. *Sci. Transl. Med.* **8**, 351ra105 (2016).

Downloaded from https://www.science.org at Fred Hutchinson Cancer Center on October 20, 2023

Science Translational Medicine

Hematopoietic stem cell transplantation in immunocompetent hosts without radiation or chemotherapy

Akanksha Chhabra, Aaron M. Ring, Kipp Weiskopf, Peter John Schnorr, Sydney Gordon, Alan C. Le, Hye-Sook Kwon, Nan Guo Ring, Jens Volkmer, Po Yi Ho, Serena Tseng, Irving L. Weissman, and Judith A. Shizuru

Sci. Transl. Med. **8** (351), . DOI: 10.1126/scitranslmed.aae0501

Make way for stem cells

Current conditioning regimens to prepare the host bone marrow for transplantation of donor hematopoietic stem cells (HSCs) can have toxic effects on the patient. As an alternative to chemotherapy or radiation, Chhabra *et al*. describe a new immunotherapy strategy that clears out host HSCs from the bone marrow in preparation for a transplant. Blockade of the surface antigen CD47 allows phagocytic myeloid cells to engulf host HSCs displaced by antibody targeting, effectively depleting HSCs from the bone marrow of immunocompetent mice. This led to improved engraftment of donor HSCs, with fewer toxic effects for the mice receiving the transplant.

View the article online
https://www.science.org/doi/10.1126/scitranslmed.aae0501
Permissions
https://www.science.org/help/reprints-and-permissions

Downloaded from https://www.science.org at Fred Hutchinson Cancer Center on October 20, 2023

Use of this article is subject to the Terms of service

Science Translational Medicine (ISSN 1946-6242) is published by the American Association for the Advancement of Science. 1200 New York Avenue NW, Washington, DC 20005. The title *Science Translational Medicine* is a registered trademark of AAAS.

Copyright © 2016, American Association for the Advancement of Science